

- er, Proc. Roy. Soc. (London) A267, 297 (1962).
- <sup>2</sup>D. R. Bates and S. P. Khare, Proc. Phys. Soc. (London) 85, 231 (1965).
- <sup>3</sup>R. Deloche, Compt. Rend. 266B, 664 (1968); and R. Deloche and A. Gonfalone, J. Phys. (Paris) 29, 27 (1968).
- <sup>4</sup>C. B. Collins, Phys. Rev. 177, 254 (1969).
- <sup>5</sup>D. R. Bates, Phys. Rev. 77, 718 (1950); 78, 492 (1950); 82, 103 (1951).
- <sup>6</sup>D. E. Kerr, Johns Hopkins University Report, 1960 (unpublished); C. S. Leffel, M. N. Hirsh, and D. E. Kerr (unpublished).
- <sup>7</sup>E. Himnov and J. G. Herschberg, Phys. Rev. 125, 795 (1962).
- <sup>8</sup>R. A. Gerber, G. F. Sauter, and H. J. Oskam, Physica 32, 217 (1966).
- <sup>9</sup>C. B. Collins and W. B. Hurt, Phys. Rev. 167, 166 (1968).
- <sup>10</sup>C. B. Collins, H. S. Hicks, and W. E. Wells, Phys. Rev. A 2, 797 (1970).
- <sup>11</sup>J. Berlande, M. Cheret, R. Deloche, A. Gonfalone, and C. Manus, Phys. Rev. A 1, 887 (1970).
- <sup>12</sup>A. W. Johnson and J. B. Gerardo, Phys. Rev. Letters, 27, 835 (1971).
- <sup>13</sup>C. B. Collins, Phys. Rev. 186, 113 (1969).
- <sup>14</sup>M. Gryzinski, Phys. Rev. 115, 374 (1949).
- <sup>15</sup>T. Holstein, Phys. Rev. 72, 1212 (1947).
- <sup>16</sup>C. B. Collins, B. W. Johnson, H. S. Hicks, and M. J. Shaw (unpublished).
- <sup>17</sup>M. A. Heald and C. B. Wharton, *Plasma Diagnostics with Microwaves* (Wiley, New York, 1965), pp. 1-10.
- <sup>18</sup>C. B. Collins and W. B. Hurt, Phys. Rev. 177, 257 (1969).
- <sup>19</sup>K. B. Persson, J. Appl. Phys. 36, 3086 (1965).
- <sup>20</sup>D. R. Bates and A. E. Kingston, Proc. Roy. Soc. (London) A279, 32 (1964).
- <sup>21</sup>R. W. Motley and A. F. Kuckes, in *Proceedings of the Fifth International Conference on Ionic Phenomena, Munich, 1961* (North-Holland, Amsterdam, 1961).

PHYSICAL REVIEW A

VOLUME 6, NUMBER 4

OCTOBER 1972

## Roton-Limited Mobility of Ions in Superfluid He<sup>4</sup>†

Ruben Barrera\* and Gordon Baym

Department of Physics, University of Illinois, Urbana, Illinois 61801

(Received 10 April 1972)

We calculate the roton-limited mobility of ions in superfluid He<sup>4</sup> for temperatures below ~1.7°K. Taking, as a first approximation, a constant ion-roton transition-matrix element, which we treat as an adjustable parameter, we find good agreement with experiment for both positive and negative ions. This model calculation indicates that the most mobile of the recently discovered "exotic" negative carriers is a very light ion.

### INTRODUCTION

The mobility of a slowly moving ion in superfluid helium is limited by collisions with the elementary excitations of the liquid. Positive and negative ions have been studied extensively in the last ten years.<sup>1-6</sup> The negative ion is an electron which creates around itself a large spherical bubble of radius ~16 Å at zero pressure; in contrast, a positive ion forms a solid helium sphere of about 6 Å radius, surrounded by high-density liquid (the "snowball" model). Very recently Ihas and Sanders<sup>7</sup> have produced new types of "exotic" negative carriers in superfluid helium, but their structure is still unknown.

At temperatures below ~0.6°K the mobility of ions is limited mainly by collisions with thermal phonons. At those temperatures mobility measurements have been successfully explained by considering the phonon-ion collision as the scattering of a classical sound wave by an elastic bubble in the case of negative ions,<sup>8</sup> and by a hard sphere in the case of positive ions.<sup>9</sup>

At higher temperatures, above ~0.8°K, the ionic mobility is limited primarily by collisions of

the ions with rotons. In the "kinetic" regime  $0.8 \lesssim T \lesssim 1.7^\circ\text{K}$  roton-roton scattering can be neglected, while above ~2°K, roton-roton scattering is so frequent that the rotons appear to the ions as a viscous fluid. Several mobility experiments<sup>10-12</sup> have been performed in the kinetic regime, and they all show a temperature dependence of the mobility  $\mu$  significantly different for positive and negative ions. The experimental results have been put in the form

$$\mu_{\pm}^{-1} \propto e^{-\Delta_{\pm}/T}, \quad (1)$$

where the subscripts  $\pm$  refer to positive and negative ions. The values found for  $\Delta_{+}$  are around 8.65-8.8°K and for  $\Delta_{-}$  around 7.7-8.1°K. Measurements of exotic negative carriers in this temperature region show that the mobility temperature dependence for the "fastest" carrier is of the form (1), but with an exponent  $\Delta^* \approx 9.6^\circ\text{K}$ . Ihas and Sanders have suggested that this carrier might represent a negative helium ion He<sup>-</sup> inside a bubble.

The exponential behavior of (1) is characteristic of the roton-dominated regime and is primarily a reflection of the temperature dependence of the

density of thermal rotons. The most simple kinetic arguments give a mobility formula in this regime

$$e/\mu = \rho_n \sigma v_{\text{rel}} \sim e^{-\Delta/T} \sigma, \quad (2)$$

where  $\rho_n$  is the roton normal mass density,  $\sim T^{-1/2} \times e^{-\Delta/T}$ ,  $\Delta$  is the roton-gap parameter,  $v_{\text{rel}} \sim T^{1/2}$  is the average relative velocity between rotons and ions, and  $\sigma$  is a mean roton-ion cross section.

While this simple picture gives a first account of the mobility, it fails to explain the differences in temperature dependence observed for positive and negative ions. These differences arise, as we shall see, when one takes into account the detailed roton-ion scattering kinematics allowing for recoil of the ions due to their finite mass.

The effective mass of the negative ion is essentially the hard-sphere hydrodynamic value  $\frac{1}{2}\rho_4 \times (\frac{4}{3}\pi a_-^3)$ , where  $a_-$  is the bubble radius, and  $\rho_4$  is the mass density of liquid He<sup>4</sup>; this mass is  $\sim 170m_4$ , where  $m_4$  is the He<sup>4</sup> atomic mass. The effective mass of the positive ion is a sum of the mass of the core,  $^3\sim 1.7\rho_4(4\pi a_+^3/3)$  (where  $a_+$  is the core radius), plus the hydrodynamic mass due to the backflow of the fluid surrounding the ion. As shown in Appendix A this mass, calculated classically, is just slightly less than the classical hydrodynamic mass  $\frac{1}{2}(\frac{4}{3}\pi a_+^3)\rho_4$  of a hard sphere. The net effective mass is  $\sim 40m_4$ . The excess mass of liquid outside the core, arising from electrostriction of the liquid by the ion, does not directly enter the effective mass needed to calculate the ionic mobility.

The problem of the roton-limited mobility of ions in He<sup>4</sup>, including effects of ionic recoil, has been considered by Bowley,<sup>13</sup> in a general formulation of the problem in terms of the van Hove scattering function of the impurities and the ion-roton scattering amplitudes. The basic problem in calculating the mobility explicitly is a lack of knowledge of the matrix elements for ion-roton scattering. Microscopic theory has not yet cast much light on this problem, though Iguchi<sup>14</sup> has given a model for scattering of rotons by fixed nonrecoiling ions via an assumed two-body potential. Two simple phenomenological approximations have been used previously: One<sup>15</sup> is to take the matrix element to be constant, while the second<sup>9</sup> is to take the square of the matrix element to be inversely proportional to the densities of initial and final roton states, so that an effective roton-ion scattering cross section is constant. For both these cases Bowley presents an expression for the mobility.

The primary purpose of this paper is to compare the predictions of simple theoretical models for the matrix elements for ion-roton scattering with the recent experiments<sup>7,11,12</sup> on the mobilities of

positive, negative, and exotic ions in superfluid He<sup>4</sup>. To do this we first, in Sec. II, present the derivation, starting from the variational principle for the ionic Boltzmann equation, of the ion mobility in the kinetic regime, in terms of the transition matrix elements for ion-roton scattering. We then discuss some considerations on the form of the matrix element and try to make contact between the several phenomenological approximations for it. Finally, in Sec. II, we give the explicit calculation of the mobility for the case of a constant  $s$ -wave transition amplitude for ion-roton scattering, and consider in a simple model the effects of momentum dependence of the transition-matrix element. The results, which for the case of a constant matrix element are mathematically the same as Bowley's, are applied to a detailed comparison with experiment in Sec. III.

## II. CALCULATION OF IONIC MOBILITY

To calculate the ionic mobility, we assume the ions to be drifting, with a mean velocity  $\vec{v}_D$ , in response to an externally applied electric field  $\vec{\mathcal{E}}$ . Through collisions of the ions with the excitations of the helium, the ions remain in a steady state transferring to the excitations the momentum gained from the field. The ionic distribution function  $f_{\vec{p}}$  is determined from the steady-state linearized Boltzmann equation

$$e\vec{\mathcal{E}} \cdot \vec{\nabla}_{\vec{p}} f_{\vec{p}}^0 = - \sum_{\vec{p}', \vec{k}, \vec{k}'} [f_{\vec{p}} n_k (1+n_{k'}) - f_{\vec{p}'} n_{k'} (1+n_k)] \times \Gamma(\vec{p}, \vec{k} \rightarrow \vec{p}', \vec{k}'), \quad (3)$$

where  $e$  is the ionic charge;

$$f_{\vec{p}}^0 = e^{-\beta p^2/2m^*} n_i (2\pi\hbar^2\beta/m^*)^{3/2} \quad (4)$$

is the equilibrium ionic distribution function, where  $n_i$  is the density of ions per unit volume,  $m^*$  is the ionic effective mass, and  $\beta = 1/\kappa T$ ;  $n_k$  is the helium excitation distribution function; and

$$\Gamma(\vec{p}, \vec{k} \rightarrow \vec{p}', \vec{k}') = \frac{2\pi}{\hbar} \delta\left(\frac{p^2}{2m^*} + \omega_k - \frac{p'^2}{2m^*} - \omega_{k'}\right) \times |\langle \vec{p}', \vec{k}' | T | \vec{p}, \vec{k} \rangle|^2 \quad (5)$$

is the rate of transitions in which an ion of momentum  $\vec{p}$  scatters to momentum  $\vec{p}'$  from an excitation of initial momentum  $\vec{k}$  and energy  $\omega_k$ , and final momentum  $\vec{k}'$  and energy  $\omega_{k'}$ .

For sufficiently low temperatures the mean free path  $l_{e-e}$  of the excitations against collisions with other excitations is  $\gg R$ , the effective radius of interaction between an excitation and an ion. In this kinetic regime, the modification of the excitation distribution function in the neighborhood of an ion can be neglected. The roton-roton collision time is given by<sup>16</sup>

$$\tau_{\text{rot-rot}}^{-1} \approx 1.3 \times 10^{13} T^{1/2} e^{-\Delta/T} \text{ sec},$$

while the mean relative roton-roton thermal velocity  $v_{\text{rot}} = (2\kappa T/\mu_r)^{1/2}$ , where  $\mu_r$  is the roton mass parameter. As we shall discuss later, the radius of interaction  $R$  is on the order of the ionic radius  $a$ ,  $\approx 6 \text{ \AA}$  for positive ions and  $\approx 16 \text{ \AA}$  for negative ions. At  $T = 1.2^\circ \text{K}$ , the roton mean free path  $l_{\text{rot-rot}} = \tau_{\text{rot-rot}} v_{\text{rot}}$  is on the order of  $170 \text{ \AA}$ ,  $\gg R$ . However, by  $T = 1.8^\circ \text{K}$ ,  $l_{\text{rot-rot}}$  becomes  $\approx 18 \text{ \AA}$ , which is on the order of the bubble radius. The assumption  $l_{\text{rot-rot}} \gg R$  is well satisfied below  $1.7^\circ \text{K}$ , but it breaks down at higher temperatures where the system enters the hydrodynamic regime.

For sufficiently small densities of ions, excitation-excitation frequencies  $\tau_{e-e}^{-1}$  are greater than excitation-ion collision frequencies  $\tau_{e-i}^{-1}$ . Thus excitation-excitation collisions bring the excitations back into thermal equilibrium, after an excitation-ion collision, before another excitation-ion collision takes place. The excitation gas dissipates the momentum gained from the ions to the walls in a characteristic time  $\tau_D$ . At sufficiently low ion densities  $\tau_D \ll \tau_{e-i}$ , so that the excitations are not dragged by the drifting ions, but rather are in equilibrium with the walls. For excitation mean free paths  $\ll L$ , the characteristic dimension of the system,  $\tau_D$  is given by the diffusion result

$$\tau_D \approx \tau_{e-e} (L/l_{e-e})^2. \quad (6)$$

Thus for

$$\tau_{e-e} (L/l_{e-e})^2 \ll \tau_{e-i}, \quad (7)$$

$n_k^0$  in Eq. (3) can be taken to be the equilibrium distribution function

$$n_k^0 = (e^{\beta\omega_k} - 1)^{-1}. \quad (8)$$

Now in the roton-ion problem we can use the estimate

$$\tau_{\text{rot-i}}^{-1} \sim v_{\text{rot}} \sigma n_i,$$

where  $\sigma \sim \pi R^2$  is a mean roton-ion cross section. Condition (7) is therefore equivalent to

$$n_i \ll l_{\text{rot-rot}}/L^2 \sigma. \quad (9)$$

Since  $L \sim 1 \text{ cm}$ , the condition for taking the excitations to be in equilibrium with the walls is  $n_i \ll 10^8 \text{ cm}^{-3}$  at  $T = 1.2^\circ \text{K}$ ; usual experimental ion densities<sup>10</sup> are  $\sim 10^6 \text{ cm}^{-3}$ .

If we now write

$$f_{\vec{p}} = (1 + \Phi_{\vec{p}}/\kappa T) f_{\vec{p}}^0 \quad (10)$$

and use the detailed balancing condition  $f_{\vec{p}}^0 n_k^0 (1 + n_k^0) = f_{\vec{p}'}^0 n_{k'}^0 (1 + n_{k'}^0)$ , the Boltzmann equation (3) becomes

$$(e^{\vec{g} \cdot \vec{p}/m^*}) f_{\vec{p}}^0 = - \sum_{\vec{p}', \vec{k}, \vec{k}'} (\Phi_{\vec{p}} - \Phi_{\vec{p}'}) f_{\vec{p}'}^0 n_k^0 (1 + n_{k'}^0) \Gamma. \quad (11)$$

The mobility is given in terms of  $\Phi_{\vec{p}}$  by

$$\vec{v}_D = \mu \vec{g} = \sum_{\vec{p}} \vec{p} \Phi_{\vec{p}} f_{\vec{p}}^0 / N_i m^* \kappa T, \quad (12)$$

where  $N_i$  is the total number of ions present.

The explicit solution of (11) for  $\Phi_{\vec{p}}$  is nontrivial; in order to calculate  $\mu$ , we turn to the variational principle for the Boltzmann equation. As is well known,<sup>17</sup> the positive structure of the kernel on the right side of (11) implies that for any trial function  $\Psi_{\vec{p}}$ ,

$$\left( \sum_{\vec{p}} \Phi_{\vec{p}} e^{\vec{g} \cdot \vec{p}/m^*} \cdot \vec{p} f_{\vec{p}}^0 / m^* \right)^{-1} = (\mu N_i \kappa T e g^2)^{-1} \leq \frac{\frac{1}{2} \sum_{\vec{p}, \vec{p}', \vec{k}, \vec{k}'} (\Psi_{\vec{p}} - \Psi_{\vec{p}'})^2 f_{\vec{p}}^0 n_k^0 (1 + n_{k'}^0) \Gamma}{\left( \sum_{\vec{p}} \Psi_{\vec{p}} e^{\vec{g} \cdot \vec{p}/m^*} \cdot \vec{p} f_{\vec{p}}^0 / m^* \right)^2}. \quad (13)$$

The right side of the inequality, evaluated for any  $\Psi_{\vec{p}}$ , is thus an upper bound on  $(\mu N_i \kappa T e g^2)^{-1}$ . We choose the simplest trial function

$$\Psi_{\vec{p}} = \vec{p} \cdot \vec{v}_D, \quad (14)$$

corresponding to the ions being in a drifting equilibrium, and find from (13) an expression (actually a lower bound) for the mobility

$$\frac{e}{\mu} = \frac{1}{6N_i \kappa T} \sum_{\vec{p}, \vec{p}', \vec{k}, \vec{k}'} (\vec{p} - \vec{p}')^2 f_{\vec{p}}^0 n_k^0 (1 + n_{k'}^0) \Gamma(\vec{p}, \vec{k} - \vec{p}', \vec{k}'). \quad (15)$$

How close is the trial function (14) to the true  $\Phi_{\vec{p}}$ ? At low temperatures where the mobility is phonon limited, this trial function becomes exact as  $m^* \rightarrow \infty$ . The mobility expression (15) reduces in this case to that derived in Ref. 8. In the roton regime, as a consequence of the roton-ion scattering kinematics, (14) will not, for general scattering amplitude  $\langle \vec{p}, \vec{k} | T | \vec{p}', \vec{k}' \rangle$ , be the exact solution in the limit  $m^* \rightarrow \infty$ . Furthermore, this limit is not realized in practice; since thermal ion momenta  $(m^* \kappa T)^{1/2}$  are on the order of typical roton momenta, ion recoil cannot be neglected. The true solution  $\Phi_{\vec{p}}$  will be of the form  $\vec{v}_D \cdot \vec{p} a(p)$ ; the mobility expression (15) will be good to the extent that the correction factor  $a(p)$  is slowly varying over the range of thermal ionic momenta.

The difficulty in evaluating the mobility (15) in the roton-limited regime is the lack of knowledge of the scattering amplitude  $\langle \vec{p}, \vec{k} | T | \vec{p}', \vec{k}' \rangle$ . To understand the expected structure of the matrix element, it is instructive for us to consider first the calculation of the cross section for a roton scattering from an ion of mass  $m^*$  initially at rest, i. e.,  $\vec{p} = 0$ . Let us assume that the matrix element  $t(k)$  for this process depends only on  $k$ , the initial roton momentum. Since the incident roton velocity is  $|\partial\omega/\partial k| = |k - k_0|/\mu_r$ , where  $k_0$  is the momentum at the roton minimum, the total cross section is given by

$$\sigma = (\mu_r / |k - k_0|) |t(k)|^2 \rho(\omega), \quad (16)$$

where  $\omega = (k - k_0)^2/2\mu_r$ , and the density of states  $\rho(\omega)$  is given by

$$\rho(\omega) = \int \frac{d^3 k'}{(2\pi\hbar)^3} \frac{2\pi}{\hbar} \delta\left(\frac{(k-k_0)^2}{2\mu_r} - \frac{(k'-k_0)^2}{2\mu_r} - \frac{(\vec{k}-\vec{k}')^2}{2m^*}\right). \quad (17)$$

Carrying out the integral we find, in the limits  $|k-k_0| \ll k_0$  and  $m^* \gg \mu_r$ , that

$$\begin{aligned} \rho(\omega) &= \frac{m^* |k-k_0|}{\pi\hbar^4} \quad (\omega \leq 2k_0^2/m^*) \\ &= \frac{m^* |k-k_0|}{\pi\hbar^4} [1 - (1 - 2k_0^2/m^* \omega)^{1/2}] \\ &\quad (\omega > 2k_0^2/m^*). \end{aligned} \quad (18)$$

The density of states peaks at the energy  $\omega = 2k_0^2/m^*$ . For  $\omega < 2k_0^2/m^*$  the cross section is given by

$$\sigma = (m^* \mu_r / \pi\hbar^4) |t(k)|^2. \quad (19)$$

We thus expect that for  $\omega \ll 2k_0^2/m^*$  the matrix element approaches a constant value

$$|t(k)| = \pi\hbar^2 R / (m^* \mu_r)^{1/2}; \quad (20)$$

then  $\sigma = \pi R^2$ , and the effective scattering length  $R$  is expected to be on the order of the ionic radius.

On the other hand, for  $\omega \gg 2k_0^2/m^*$  corresponding to extremely massive ions, we have

$$\sigma = (\mu_r k_0^2 / \pi\hbar^4 \omega) |t(k)|^2. \quad (21)$$

If the cross section is constant in this regime, say  $\sigma = \pi R_1^2$ , then one would expect

$$|t(k)| = \frac{\pi\hbar^2 R_1}{\mu_r} \frac{|k-k_0|}{2^{1/2} k_0}. \quad (22)$$

This limit is that considered by Iguchi<sup>14</sup>; in his model for scattering of rotons by fixed ( $m^* \rightarrow \infty$ ) ions via a two-body potential  $V(r)$ , the  $|k-k_0|$  dependence of  $t(k)$  arises from the fact that the density of intermediate states in the roton-ion potential scattering behaves as  $|k-k_0|^{-1}$ , as in (18) when  $m^* \rightarrow \infty$ . One cannot infer, however, from his calculation how to generalize the matrix element to the case of recoiling ions ( $m^*$  finite).

Generally, one might expect the matrix element to have a structure similar to

$$|t(k)|^2 = \frac{\pi^2 \hbar^4}{m^* \mu_r} \left( R^2 + R_1^2 \frac{|k-k_0|^2}{2k_0^2} \frac{m^*}{\mu_r} \right). \quad (23)$$

A first-principles calculation of the complete matrix element  $\langle \vec{p}\vec{k} | T | \vec{p}'\vec{k}' \rangle$  represents a challenging theoretical problem. In the following we shall explicitly calculate the mobility assuming that the matrix element is given simply by the constant value (20) or, equivalently,

$$\langle \vec{p}, \vec{k} | T | \vec{p}', \vec{k}' \rangle = \frac{\pi\hbar^2 R}{(m^* \mu_r)^{1/2} \Omega} \delta_{\vec{p}+\vec{k}, \vec{p}'+\vec{k}'}, \quad (24)$$

where  $\Omega$  is the volume of the system;  $R$  shall be fitted to experiment. As we shall see from this fitting,  $R \approx 9.81 \text{ \AA}$  for positive ions and  $18.65 \text{ \AA}$  for negative ions (values close to the ionic radii). We shall also consider more qualitatively the effects of a momentum-dependent term in  $T$ , such as the  $R_1^2$  term in (23). We turn then to the calculation of the mobility using (24) and (15).

Rotons can be described by Boltzmann statistics, and thus  $n_k^0$  in (15) can be neglected and  $n_k^0$  replaced by  $e^{-\beta\omega_k}$ , where

$$\omega_k = \Delta(T) + (k-k_0)^2/2\mu_r$$

is the roton energy. The roton-gap parameter  $\Delta$  depends on  $T$ , as do  $k_0$  and  $\mu_r$ . The mobility (15) then becomes

$$\frac{e}{\mu} = \frac{\pi^3 R^2}{3\kappa T m^* \mu_r \hbar^3} \int \frac{d^3 k}{(2\pi)^3} \frac{d^3 k'}{(2\pi)^3} (\vec{k}-\vec{k}')^2 n_k^0 S(\vec{k}, \vec{k}'); \quad (25)$$

following Bowley<sup>13</sup> and Josephson and Lekner<sup>18</sup> we have introduced the function

$$S(\vec{k}, \vec{k}') = \frac{1}{N_i} \sum_{\vec{p}} f_{\vec{p}}^0 \delta\left(\frac{p^2}{2m^*} + \omega_k - \frac{(\vec{p}+\vec{k}-\vec{k}')^2}{2m^*} - \omega_{k'}\right). \quad (26)$$

$S$  is readily calculated by first exponentiating the energy delta function; then the  $\vec{p}$  summation gives

$$\begin{aligned} S(\vec{k}, \vec{k}') &= \left( \frac{m^* \beta}{2\pi |k-k'|^2} \right)^{1/2} \\ &\times \exp\left[ -\frac{\beta m^*}{2 |k-k'|^2} \left( \omega_k - \omega_{k'} - \frac{(\vec{k}-\vec{k}')^2}{2m^*} \right)^2 \right]. \end{aligned} \quad (27)$$

The calculation of the mobility is reduced to a straightforward integration:

$$\begin{aligned} \frac{e}{\mu} &= \left( \frac{\pi^5 \beta^3}{2m^*} \right)^{1/2} \frac{R^2}{3\hbar^3 \mu_r (2\pi)^6} \int d^3 k d^3 k' |\vec{k}-\vec{k}'| \\ &\times \exp\left[ -\beta \left( \frac{\omega_k + \omega_{k'}}{2} + \frac{m^*(\omega_k - \omega_{k'})^2}{2 |k-k'|^2} + \frac{(\vec{k}-\vec{k}')^2}{8m^*} \right) \right]. \end{aligned} \quad (28)$$

We carry out the explicit integration in Appendix B and find the final result

$$\frac{e}{\mu} = \frac{4}{3} (2\pi)^{1/2} \rho_n v_{\text{rot}} R^2 F(\beta k_0^2/4m^*); \quad (29)$$

here

$$\rho_n = \frac{k_0^4}{3\pi \hbar^3} \left( \frac{\mu_r \beta}{2\pi} \right)^{1/2} e^{-\beta\Delta(T)} \quad (30)$$

is the roton normal mass density,  $v_{\text{rot}} = (\beta\mu_r)^{-1/2}$  is the mean roton velocity, and

$$F(z) = z^{-1} + e^{-z} [zK_0(z) - (1+z)K_1(z)], \quad (31)$$

where  $K_n(z)$  is the Bessel function of imaginary argument of order  $n$  (and  $K_1 = -\partial K_0/\partial z$ ).

The temperature dependence of  $(e/\mu) e^{\beta\Delta(T)}$  is contained entirely in the function  $F(\beta k_0^2/2m^*)$  in

this model calculation. As a consequence, the temperature dependence of the mobility (29) depends, as observed experimentally, on the ionic effective mass. The function  $F(z)$  has a single maximum at  $z \approx 0.60$ , while for small  $z$ ,

$$F(z) = -z \left( \frac{3}{2} - z \right) (\gamma + \log_{10} \frac{1}{2} z) + \frac{3}{4} z + \dots, \quad (32)$$

where  $\gamma = 0.5772157$  is Euler's constant. This latter expression for  $F$  is accurate over the range of experimental interest for positive and negative ions ( $z = 11.1/m^* T$ , where  $m^*$  is measured in  $\text{He}^4$  masses and  $T$  in  $^\circ\text{K}$ ). In the temperature range  $1.0 < T < 1.7^\circ\text{K}$ ,  $F(z)$  decreases with  $T$  in the case of heavy ions ( $m^* \gg 15m_4$ ) and increases with  $T$  for light ions ( $m^* \ll 15m_4$ ). As will be seen in Fig. 1, the slope of  $\log_{10}[(e/\mu)e^{\beta\Delta(T)}]$ , as a function of  $T$ , decreases with increasing effective mass.

As  $z \rightarrow 0$ ,  $F(z) \rightarrow 0$  as  $-\frac{3}{2}z \log_{10} \frac{1}{2} z$ . This would imply an infinite mobility in the case of infinitely massive ions. The problem here is the neglect of momentum dependent terms in the matrix element. The source of the logarithm can be seen in the density-of-states factor  $\rho(\omega)$  [Eq. (18)] in the limit  $m^* \rightarrow \infty$ ; there  $\rho(\omega) \sim 1/|k - k_0|$ . The integration of this density of states times a constant matrix element (squared) has a logarithmic singularity at  $k = k_0$ . In order to study the effect of momentum-dependent terms in  $|\langle \vec{p}\vec{k} | T | \vec{p}'\vec{k}' \rangle|^2$  we calculate with a simple model expression, analogous to (23),

$$|\langle \vec{p}, \vec{k} | T | \vec{p}', \vec{k}' \rangle|^2 = \frac{\pi^2 \hbar^4}{m^* \mu_r \Omega} \times \left( R^2 + R_1^2 \frac{[\frac{1}{2}(k+k') - k_0]^2}{2k_0^2} \frac{m^*}{\mu_r} \right) \delta_{\vec{p}+\vec{k}, \vec{p}'+\vec{k}'}. \quad (33)$$

This approximation is symmetric in  $\vec{k}$  and  $\vec{k}'$ . The calculation of  $e/\mu$  proceeds as before, with the result

$$e/\mu = \frac{4}{3} (2\pi)^{1/2} \rho_n v_{\text{rot}} [R^2 F(z) + R_1^2 F_1(z)], \quad (34)$$

where

$$F_1(z) = \frac{1}{10} z^{-2} - \frac{1}{10} e^{-z} [(3z + \frac{1}{2}) K_0 - (3z - 1 - z^{-1}) K_1]. \quad (35)$$

The calculation of  $F_1$  is analogous to that of  $F$  given in Appendix B; the integration involves simply an extra factor  $\nu^2$  in the integrand in (B4). For small  $z$  we find

$$F_1(z) = -\frac{1}{6} F(z) + \frac{3}{8} - \frac{5}{24} z + \dots \quad (36)$$

The mobility then approaches a finite limit  $\sim R_1^{-2}$  as  $m^* \rightarrow \infty$ :

$$e/\mu \rightarrow (\frac{1}{2}\pi)^{1/2} R_1^2 \rho_n v_{\text{rot}}, \quad (37)$$

similar to the simple form (2).

### III. COMPARISON WITH EXPERIMENT

In evaluating the mobility we parametrize the temperature dependence of the roton minimum  $\Delta(T)$  as follows. The temperature dependence of

the roton energy arises as a consequence of both the thermal expansion of the medium as well as the interaction of the given roton with the thermal rotons. This latter interaction gives rise to an energy, in the sense of the Landau-Fermi liquid theory, equal to  $fn_r(T)$ , where  $f$  is the effective  $s$ -wave roton-roton interaction and  $n_r \propto T^{1/2} e^{-\beta\Delta(T)}$  is the number of thermal rotons per unit volume.<sup>19</sup> The thermal expansion changes the roton energy by an amount

$$\left( \frac{\partial \Delta}{\partial T} \right)_{\text{exp}} = \frac{\partial \Delta}{\partial \rho} \frac{\partial \rho}{\partial T},$$

where  $\rho$  is the density. To a first approximation,  $\partial \rho / \partial T$  in the roton region is given by  $-\rho(\partial \Delta / \partial \rho) \times (\partial n_r / \partial T) / m_4 s^2$ , where  $s$  is the first sound velocity. Thus the roton energy can be written in the approximate form

$$\Delta(T) = \Delta(0) + \left[ f - \frac{\rho}{m_4 s^2} \left( \frac{\partial \Delta}{\partial \rho} \right)^2 \right] n_r. \quad (38)$$

Since  $n_r$  depends on  $\Delta(T)$  this is actually an equation for  $\Delta(T)$ . Fitting this form to recent neutron scattering data of Woods<sup>20</sup> we find

$$\Delta(T) = 8.68 - 35.63 T^{1/2} e^{-\Delta(T)/T}, \quad (39)$$

where  $\Delta$  and  $T$  are in  $^\circ\text{K}$ . We generate  $\Delta(T)$  for  $T < 2.05^\circ\text{K}$  from this equation; at higher temperatures we take  $\Delta(T)$ , when used, directly from the neutron scattering data of Henshaw and Woods.<sup>21</sup>

In the actual computation of the integrals in (28) used here, we have taken into account the asymmetry of the roton spectrum about the minimum  $k_0$  by writing

$$\omega_k = \Delta_0 + (k - k_0)^2 / 2\mu_r + \Delta_3 (k - k_0)^3 + \Delta_4 (k - k_0)^4 \quad (40)$$

in the neighborhood of  $k_0$ . The values of  $\mu_r$ ,  $\Delta_3$ , and  $\Delta_4$  have been calculated<sup>22</sup> using a least-squares fit to the recent Woods data<sup>20</sup>:  $\mu_r = 0.154m_4$ ,  $\Delta_3 = (19.73/\hbar^2) (^\circ\text{K} \text{ \AA}^3)$ , and  $\Delta_4 = -(80.34/\hbar^4) (^\circ\text{K} \text{ \AA}^4)$ .

For thermal rotons at  $T = 1.5^\circ\text{K}$  the corrections to the parabolic spectrum are  $\sim 10\%$ ; the corrections here to  $F(z)$  are  $\sim +8.2\%$  for negative ions and  $\sim +13.5\%$  for positive ions; the corrections increase with increasing  $T$ . To calculate these corrections it is only necessary to expand (28) to first order in  $\Delta_4$  and second order in  $\Delta_3$ .

To compare the calculated roton mobility with experiment we must first estimate the contribution of the phonons in limiting the mobility. Phonons and rotons contribute additively to  $\mu^{-1}$ . The phonon contribution to the inverse mobility is given by<sup>8</sup>

$$\left( \frac{e}{\mu} \right)_{\text{ph}} = - \int_0^\infty \frac{dk k^4}{6\pi^2 \hbar^3} \frac{\partial n_k}{\partial k} \sigma_T(k), \quad (41)$$

where  $n_k = (e^{\beta \epsilon_k} - 1)^{-1}$  and  $\sigma_T(k)$  is the momentum-

transfer cross section. For positive ions we take the cross section to be given by the mean value  $240 \text{ \AA}^2$ ,<sup>9</sup> while for negative ions we use the more detailed cross section given in Ref. 8, taking as parameters there  $a = 17.0 \text{ \AA}$ ,  $\gamma_0 = 4.26$ , and  $\gamma_2 = 1.10$ ; these parameters fit the recent low-temperature mobility data of Schwarz<sup>12</sup> to within 5%. Comparison of the calculated phonon mobilities with experiment shows that for negative ions the contribution of  $\mu_{\text{ph}}^{-1}$  to the total inverse mobility  $\mu^{-1}$  is about 8% at  $0.8^\circ\text{K}$  dropping to 2% at  $1.0^\circ\text{K}$ ; for temperatures as high as  $1.7^\circ\text{K}$ , it is only 0.5%.

We show in Fig. 1 the experimental inverse mobility, times  $e^{\beta\Delta(T)}$ , as taken from the most recent data of Schwarz,<sup>12</sup> Brody,<sup>11</sup> and Kuchnir,<sup>23</sup> as well as the data of Ihas and Sanders<sup>7</sup> for their fastest negative exotic carrier;  $\Delta(T)$  is taken from Eq. (39). The inverse mobility data with the phonon contribution subtracted out (when the correction is noticeable) are shown as black dots immediately below the corresponding data points of Schwarz.

The solid lines in the figure are calculated from Eq. (31), taking  $m^* = 170m_4$  for negative ions and  $40m_4$  for positive ions, and fitting the scattering length  $R$  by making the theoretical and experimental values coincide at  $T = 1.2^\circ\text{K}$ . This gives the values  $R_+ = 9.18 \text{ \AA}$  for positive ions and  $R_- = 18.65 \text{ \AA}$  for negative ions, values quite close to the geometric size of the ions. In the kinetic regime  $T < 1.7^\circ\text{K}$ , the agreement between theory and experiment is better than 10%. The model gives the observed steeper slope for negative ions, compared with positive ions.

The discrepancies between the model and experiment can in part be attributed to momentum-dependent terms in the scattering-matrix element. As can be seen from the sample form [Eq. (33)] for  $|T|^2$ , the momentum-dependent terms should increase the scattering at larger roton energies, i. e., higher  $T$ . This tends to flatten out the  $m^* = 170$  and  $40$  curves towards higher  $T$ . We have from (34) and (36) in this case

$$\frac{e}{\mu} \sim (R^2 - \frac{1}{8}R_1^2) F\left(\frac{11.1}{m^*T}\right) + \frac{3}{8}R_1^2 \left(1 - \frac{6.17}{m^*T}\right), \quad (42)$$

with  $T$  in  $^\circ\text{K}$  and  $m^*$  measured in  $\text{He}^4$  masses. We have not attempted to do a precise fit to the data using this form, since the uncertainties in the roton-limited-mobility data points in Fig. 1, together with the uncertainties in the structure of the momentum-dependent terms in the matrix element, makes an accurate fitting lose its significance. Such a fit awaits a better theoretical model for the roton-ion scattering-matrix elements.

At higher temperatures the kinetic theory is no longer valid because hydrodynamic-collision effects begin to be important; the calculation of the ionic mobility between  $\sim 1.7$  and  $2.0^\circ\text{K}$  would re-

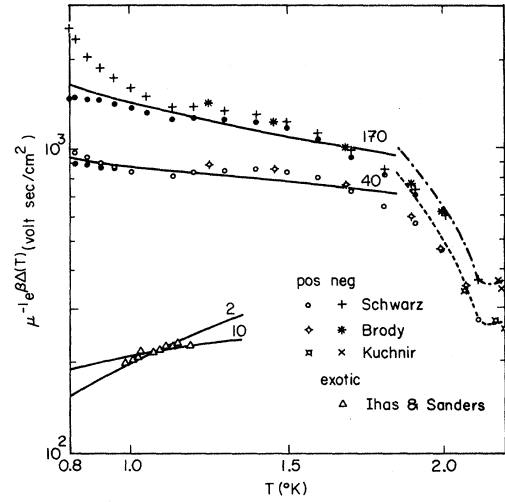


FIG. 1. Calculated roton-limited mobilities. The solid curve labeled 170 is for negative ions with  $m^* = 170m_4$  and  $R = 18.65 \text{ \AA}$ ; the solid curve labeled 40 is for positive ions with  $m^* = 40m_4$  and  $R = 9.81 \text{ \AA}$ ; the solid curve labeled 2 corresponds to  $m^* = 2m_4$  and  $R = 8.86 \text{ \AA}$ ; and the solid curve labeled 10 corresponds to  $m^* = 10m_4$  and  $R = 4.65 \text{ \AA}$ . The broken curves represent the Stokes mobilities as calculated in Ref. 24; the dashed curve is for the positive ion and the dash-dot curve is for the negative ion. With the exception of the black dots the rest of the symbols correspond to data points. As discussed in the text the black dots are the result of subtracting the phonon contribution from the data of Schwarz (Ref. 12); they lie directly below their corresponding data points.

quire a more general solution of the Boltzmann equation. At  $2.0^\circ\text{K}$  the system reaches the Stokes regime; we show as dotted curves in the figure the Stokes-law mobility calculation of Dahm and Sanders.<sup>24</sup>

We consider briefly the possible errors in the data points as shown in the figure. The accuracy of the mobility measurements of Schwarz, Brody, and Ihas and Sanders is  $\sim 3\%$ , while that of Kuchnir is accurate to within 10%. The neutron scattering data from which  $\Delta(T)$  is determined is accurate, for example, to 4% at  $T \sim 1.5^\circ\text{K}$ . The total error in  $\mu^{-1}e^{\beta\Delta(T)}$  can thus be  $\sim 6\%$  at  $1.5^\circ\text{K}$ ; similarly one finds a cumulative error  $\sim 4\%$  at  $T = 1^\circ\text{K}$ . The deviations between theory and experiment go the same way with temperature for both positive and negative ions; this could arise from an error in  $\Delta(T)$ .

The error in the determination of the phonon-limited mobility is important only for negative ions at  $T \lesssim 1^\circ\text{K}$ . For example, at  $T = 0.8^\circ\text{K}$  the phonon contribution to the mobility is  $\sim 40\%$ ; thus even an error as big as 10% in  $\mu_{\text{ph}}^{-1}$  will produce an error of  $\sim 4\%$  in  $\mu_{\text{rot}}^{-1}$ . At higher temperatures, say  $1^\circ\text{K}$ , the phonon contributions drop down to 15%; thus a 10% error in  $\mu_{\text{ph}}^{-1}$  will produce an error of only 1.5%

in  $\mu_{\text{rot}}^{-1}$ .

The temperature dependence of the ionic radius and hence  $m^*$  (for  $T < 1.7^\circ\text{K}$ ) gives rise to changes in the calculated mobility of less than 1% for both kinds of ions. A choice of a smaller ionic mass gives a better fit to experiment for both types of ions; however, this seems inconsistent with presently accepted ionic models.

There is still no model for the structure of the exotic negative carriers. The mobility measurements cover only a small temperature region ( $0.95 < T < 1.2^\circ\text{K}$ ) and show that  $\mu^{-1} e^{\beta\Delta(T)}$  increases with temperature. This is consistent with the behavior of the calculated mobility in the case of very light ions ( $m^* < 15m_4$ ). In Fig. 1 we show a plot of the calculated  $(e/\mu) e^{\beta\Delta(T)}$  for effective ionic masses of 2 and  $10m_4$  with corresponding values of  $R$  of 8.86 and 4.65 Å. The results are in agreement with the experiment within the measured temperature region. Extension of the measurements to a wider temperature range are clearly needed.

#### ACKNOWLEDGMENTS

We wish to thank Professor Klaus Schwarz and Dr. G. Ihas for providing us with data prior to publication. Helpful conversations with Professor C. J. Pethick were much appreciated.

#### APPENDIX A: CALCULATION OF HYDRODYNAMIC MASS OF POSITIVE He<sup>+</sup> ION

In this appendix we calculate classically the hydrodynamic mass of the positive helium-ion snowball moving in superfluid helium with slow velocity  $\vec{u}$ . We characterize the snowball as a solid core of radius  $a$  plus a polarization potential  $\Phi(\vec{r})$ , which exerts an attractive force in the fluid producing an increase in density in the surrounding liquid.

The snowball hydrodynamic mass  $m_H^*$  is given by one-half the coefficient of  $u^2$  in the expansion of the total fluid energy  $E$  in the presence of the moving snowball. By symmetry the linear term vanishes and we have

$$E = E_0 + \frac{1}{2} m_H^* u^2 + \dots, \quad (\text{A1})$$

where  $E_0$  is the fluid energy with the snowball at rest. The total energy of the liquid can be written as

$$E = \int d^3r \left[ \frac{1}{2} m n'(\vec{r}) v(\vec{r})^2 + \mathcal{S}'(\vec{r}) + n'(\vec{r}) \Phi(\vec{r}) \right], \quad (\text{A2})$$

where  $m$  is the He<sup>4</sup> mass,  $n'(\vec{r})$  is the fluid number density,  $\vec{v}(\vec{r})$  is the fluid velocity field, and  $\mathcal{S}'(\vec{r})$  is the fluid internal energy in the presence of the moving snowball;  $n' \Phi$  is the electrical contribution to the fluid energy due to the polarization potential. We denote by  $n(\vec{r})$  and  $\mathcal{S}(\vec{r})$  the number and internal energy density of the fluid were the snowball at rest at its instantaneous position at time  $t$ . Then

to second order

$$E - E_0 = \int d^3r \left( \frac{1}{2} m n(\vec{r}) v(\vec{r})^2 + [\mu(\vec{r}) + \Phi(\vec{r})] [n'(\vec{r}) - n(\vec{r})] + \frac{1}{2} \frac{\partial \mu}{\partial n}(\vec{r}) [n'(\vec{r}) - n(\vec{r})]^2 \right), \quad (\text{A3})$$

where  $\mu = \partial \mathcal{S} / \partial n$  is the fluid chemical potential. However, in thermodynamic equilibrium the total chemical potential  $\mu(\vec{r}) + \Phi(\vec{r}) = \mu_\infty$  is constant everywhere in space; thus the term  $\sim \mu_\infty$  in (A3) vanishes since the integrals of  $n(\vec{r})$  and  $n'(\vec{r})$  over all space both equal the total number of particles in the system.

The fluid hydrodynamic equations are

$$\frac{\partial n'(\vec{r}, t)}{\partial t} + \vec{\nabla} \cdot [n'(\vec{r}, t) \vec{v}(\vec{r}, t)] = 0, \quad (\text{A4})$$

$$m \left( \frac{\partial \vec{v}(\vec{r}, t)}{\partial t} + [\vec{v}(\vec{r}, t) \cdot \vec{\nabla}] \vec{v}(\vec{r}, t) \right) = - \vec{\nabla} [\mu'(\vec{r}, t) + \Phi(\vec{r}, t)]. \quad (\text{A5})$$

For uniform motion of the snowball,  $\vec{v}(\vec{r}, t) = v(\vec{r} - \vec{u}t, 0)$ ; thus the left side of (A5) is second order in  $\vec{u}$ . To first order in  $\vec{u}$ ,

$$\vec{\nabla} [\mu'(\vec{r}, t) + \Phi(\vec{r}, t)] = \vec{\nabla} \left( \mu_\infty + \frac{\partial \mu}{\partial n}(\vec{r}) [n'(\vec{r}, t) - n(\vec{r}, t)] \right) = 0.$$

This means that  $(\partial \mu / \partial n)(n' - n)$  must be constant everywhere in space; but since at infinity  $n' = n$ , this constant must be zero. The change in density  $n' - n$  is therefore second order in  $u$  (as is apparent from symmetry considerations) and it can therefore be neglected in (A3). The second-order contribution to  $E - E_0$  is simply  $\int \frac{1}{2} m n(\vec{r}) v(\vec{r})^2$ .

To calculate  $\vec{v}(\vec{r})$  to first order in  $u$  we observe that for uniform motion  $n'(\vec{r}, t) = n'(\vec{r} - \vec{u}t, 0)$ , so that (A4) becomes

$$\vec{\nabla} \cdot \{n(\vec{r}, t) [v(\vec{r}, t) - \vec{u}]\} = 0. \quad (\text{A6})$$

The boundary conditions on this equation are that at the surface of the hard core of the snowball at radius  $a$ , the component of  $\vec{v} - \vec{u}$  normal to the surface vanishes, while  $\vec{v}(\vec{r}) \rightarrow 0$  at  $\infty$ . The solution to (A6) is given in terms of the classical hard-sphere solution by

$$n(\vec{r}) [\vec{v}(\vec{r}) - \vec{u}] = n_0 [\vec{v}_{\text{HS}}(\vec{r}) - \vec{u}], \quad (\text{A7})$$

where

$$\vec{v}_{\text{HS}}(\vec{r}) = (a^3/2r^3) (3\hat{r}(\vec{u} \cdot \hat{r}) - \vec{u}) \quad (r \geq a) \quad (\text{A8})$$

is the flow produced by a hard sphere (when instantaneously at the origin) and  $n_0$  is the fluid density at infinity. Thus, from (A7),

$$\vec{v}(\vec{r}) = \frac{n_0}{n(r)} \vec{v}_{\text{HS}}(\vec{r}) + \left(1 - \frac{n_0}{n(r)}\right) \vec{u}. \quad (\text{A9})$$

Substituting (A9) into  $\frac{1}{2}m \int n(r) v(r)^2 d^3r$  and doing the angular average, we find the result for the hydrodynamic mass of the ion:

$$\frac{m_H^*}{m} = \int_a^\infty d^3r \left[ \frac{n_0^2}{n(r)} \frac{a^6}{2r^6} + n(r) \left(1 - \frac{n_0}{n(r)}\right)^2 \right]. \quad (\text{A10})$$

In order to estimate  $m_H^*$ , we note that to a first approximation the density profile  $n(r)$  for a snowball at rest<sup>1</sup> is given by

$$n(r) - n_0 = (n_m - n_0) (a/r)^4 \equiv \lambda n_0 (a/r)^4, \quad (\text{A11})$$

where  $n_m = n(a)$  is the equilibrium density of liquid He<sup>4</sup> at the solidification pressure. With (A11), the expression for the hydrodynamic mass becomes

$$\frac{m_H}{m} = 4\pi a^3 n_0 \int_1^\infty \frac{dx}{x^4 + \lambda} \left( \frac{1}{2} + \frac{\lambda^2}{x^2} \right). \quad (\text{A12})$$

While the integration is straightforward, it is sufficient to expand (A12) for small  $\lambda$ ; then

$$m_H/m = (m_{\text{HS}}/m) \left(1 - \frac{3}{7}\lambda + \frac{81}{55}\lambda^2 - \frac{13}{15}\lambda^3 \pm \dots\right), \quad (\text{A13})$$

where  $m_{\text{HS}} = \frac{2}{3}\pi a^3 n_0 m$  is the hydrodynamic mass of a hard sphere of radius  $a$ . Taking  $\lambda = 0.186$ ,<sup>25</sup> we find  $m_H = 0.97m_{\text{HS}}$ , a reduction of about  $0.3m$ .

The total effective mass of the positive ion is then the mass of the hard core plus the hydrodynamic term  $m_H$ . One should note that the mass excess

$$m \int_0^\infty d^3r [n(r) - n_0] \approx 6\lambda m_{\text{HS}}$$

outside the hard core does not contribute directly to the effective mass, since the excess He<sup>4</sup> particles outside the core do not travel with the core at velocity  $\vec{u}$ . The hydrodynamic mass is reduced from its hard-sphere value, since the increased fluid density near the ion causes the flow velocity, and hence the fluid kinetic energy, to be reduced.

#### APPENDIX B: INTEGRATION OF ROTON-MOBILITY FORMULA

In this appendix we show the integration procedure used to obtain Eq. (29) from (28). We first define in the integral in (28) the variable  $x$  by

$$(\vec{k} - \vec{k}')^2 = 8m^* x/\beta; \quad (\text{B1})$$

the range of  $x$  is  $\beta(k - k')^2/8m^* \leq x \leq \beta(k + k')^2/8m^*$ . Then we introduce the variables  $\lambda$  and  $\nu$  by writing

$$\frac{1}{2}(k - k') = \lambda(2\mu/\beta)^{1/2}, \quad \frac{1}{2}(k + k') = k_0 + \nu(2\mu/\beta)^{1/2}. \quad (\text{B2})$$

With these variables Eq. (28) becomes

$$e/\mu = (4k_0^4 R^2/9\pi\hbar^3) e^{-\beta\Delta(T)} F(z), \quad (\text{B3})$$

where

$$F = \frac{3}{4\pi^{1/2}z} \int_{-\infty}^{\infty} d\lambda \int_{-1/y}^{\infty} d\nu [(1 + \nu y)^2 - \lambda^2 y^2] \times e^{-(\nu^2 + \lambda^2)} \int_{\lambda^2 \mu_r/m^*}^{2x(1+\nu y)^2} dx x^{1/2} e^{-x - \lambda^2 \nu^2/x}, \quad (\text{B4})$$

$$y = (2\mu_r/\beta k_0^2)^{1/2}, \quad (\text{B5})$$

and

$$z = \beta k_0^2/4m^*. \quad (\text{B6})$$

For all temperatures of interest  $y$  is  $\ll 1$ ; then because of the Gaussian  $e^{-(\nu^2 + \lambda^2)}$ , the terms  $\nu y$  and  $\lambda^2 y^2$  may be safely neglected in (B4), the lower limit of the  $\nu$  integration may be replaced by  $-\infty$ , and since  $\mu_r/m^* \ll 1$ , the lower limit of the  $x$  integration may be replaced by zero. Thus doing the  $\nu$  integration, we find

$$F = \frac{3}{2z} \int_0^\infty d\lambda \int_0^{2x} dx \frac{x e^{-(x+\lambda^2)}}{(x+\lambda^2)^{1/2}}. \quad (\text{B7})$$

If we now let  $\lambda = ax^{1/2}$  and do the  $x$  integration, we find

$$F(z) = \frac{1}{z} - \frac{3}{2z} e^{-2z} \int_0^\infty \frac{da}{(1+z^2)^{5/2}} e^{-2za^2} (1+2z+2za^2). \quad (\text{B8})$$

Using

$$b^{-5/2} = \frac{8}{3\pi^{1/2}} \int_0^\infty dw w^4 e^{-w^2 b}$$

and the integral representation of the Bessel function<sup>26</sup>

$$K_0(z) = 2e^{-z} \int_0^\infty dw e^{-2zw^2} (1+w^2)^{-1/2},$$

we have

$$F(z) = \frac{1}{z} - ze^{-2z} \left( \frac{\partial^2}{\partial z^2} - 3 \frac{\partial}{\partial z} \right) [e^z K_0(z)].$$

Then employing the Bessel equation  $K_0'' + K_0'/z - K_0 = 0$ , and the relation  $K_1 = -K_0'$ , we derive Eqs. (29) and (31).

<sup>†</sup>Research supported in part by the Advanced Research Project Agency under Contract No. ARPA SD-131 and by the National Science Foundation under Grant No. NSF GP-16886.

\*Present address: Battelle-Institut ev, 6 Frankfurt 90, Postfach 900160, West Germany.

<sup>1</sup>K. R. Atkins, Phys. Rev. **116**, 1339 (1959).

<sup>2</sup>L. Meyer and F. Reif, Phys. Rev. Letters **5**, 1 (1960).

<sup>3</sup>A. Dahm and T. M. Sanders, Phys. Rev. Letters **17**, 126 (1966); J. Low Temp. Phys. **2**, 199 (1970).

<sup>4</sup>R. G. Arkhipov, Usp. Fiz. Nauk **88**, 185 (1966) [Sov. Phys. Usp. **9**, 174 (1966)].

<sup>5</sup>S. Wang, Ph. D. thesis (University of Michigan, 1967) (unpublished).

<sup>6</sup>K. W. Schwarz and R. W. Stark, Phys. Rev. Letters **21**, 967 (1968).

<sup>7</sup>G. G. Ihas and T. M. Sanders, Phys. Rev. Letters **27**, 383 (1971).

<sup>8</sup>G. Baym, R. G. Barrera, and C. J. Pethick, Phys. Rev. Letters **22**, 20 (1969).



- <sup>9</sup>K. W. Schwarz and R. W. Stark, *Phys. Rev. Letters* **22**, 1278 (1969).
- <sup>10</sup>F. Reif and L. Meyer, *Phys. Rev.* **119**, 1164 (1960).
- <sup>11</sup>B. A. Brody, Ph.D. thesis (University of Michigan, 1970) (unpublished).
- <sup>12</sup>K. W. Schwarz (unpublished).
- <sup>13</sup>R. M. Bowley, *J. Phys. C* **4**, 853 (1971); **4**, 1645 (1971).
- <sup>14</sup>I. Iguchi, *J. Low Temp. Phys.* **4**, 637 (1971).
- <sup>15</sup>I. M. Khalatnikov and V. Zharkov, *Zh. Eksperim. i Teor. Fiz.* **32**, 1108 (1957) [*Sov. Phys. JETP* **5**, 905 (1957)].
- <sup>16</sup>See, for example, I. M. Khalatnikov, *Introduction to the Theory of Superfluidity* (Benjamin, New York, 1965), Chap. VII.
- <sup>17</sup>For example, J. M. Ziman, *Electrons and Phonons* (Oxford U.P., Oxford, England, 1960), p. 278.
- <sup>18</sup>B. D. Josephson and J. Lekner, *Phys. Rev. Letters* **23**, 111 (1969).
- <sup>19</sup>J. Ruvalds, *Phys. Rev. Letters* **27**, 1769 (1971); G. Baym and D. Pines (unpublished).
- <sup>20</sup>A. D. B. Woods (unpublished).
- <sup>21</sup>D. G. Henshaw and A. D. B. Woods, *Phys. Rev.* **121**, 1266 (1961).
- <sup>22</sup>We are grateful to Mr. D. M. Saul for assistance with this calculation.
- <sup>23</sup>M. Kuchnir, Ph.D. thesis (University of Illinois, 1966) (unpublished).
- <sup>24</sup>We take the Stokes-law mobility calculation from Ref. 3 but we normalize the data with the experimental points of Ref. 23 rather than with the measurements of Ref. 10.
- <sup>25</sup>W. H. Keesom, *Helium* (Elsevier, Amsterdam, 1942), p. 237.
- <sup>26</sup>I. S. Gradshteyn and I. M. Ryzhik, *Table of Integrals, Series, and Products* (Academic, New York, 1965), p. 316.

## Self-Defocusing of Light by Adiabatic Following in Rubidium Vapor

D. Grischkowsky and J. A. Armstrong\*

*IBM Thomas J. Watson Research Center, Yorktown Heights, New York 10598*

(Received 3 March 1972)

The narrow-line output of a dye laser on the low-frequency side of the  $^2P_{1/2}$  resonance line (7948 Å) of rubidium was self-defocused by passage through dilute rubidium vapor. The defocusing was caused by the electronic nonlinearity associated with "adiabatic following" of the laser field by the pseudomoment of the resonant atoms. By using the corresponding nonlinear dielectric constant, the wave equation was solved numerically and gave excellent quantitative agreement with experiment.

### INTRODUCTION

In the experiments on thermal self-defocusing of light, the intensity dependence of the dielectric constant  $\epsilon$  was due to absorption and subsequent heating.<sup>1-3</sup> The self-defocusing reported here is due to the resonant nonlinearity associated with adiabatic following, and the observations provide a precise test of the adiabatic following model.

Previously, Grischkowsky<sup>4</sup> observed the self-focusing of light by potassium vapor when the frequency  $\nu$  of the light was greater than the frequency  $\nu_0$  of the  $^2P_{3/2}$  resonance line (7665 Å) of potassium; however, when  $\nu < \nu_0$ , no self-focusing was observed. Instead the observations were consistent with self-defocusing. These results could be explained either by the adiabatic following model, which was introduced in Ref. 4, or by the steady-state model of Javan and Kelley.<sup>5</sup> Both models give constitutive relations which are local and known analytically for all intensities. Also, the resonant electronic nonlinearity of each model causes self-focusing when  $\nu_0 < \nu$  and self-defocusing when  $\nu < \nu_0$ . Recently, Akhmanov *et al.*<sup>6</sup> observed self-focusing and self-defocusing in potas-

sium vapor. In a limited region they were able to show experimentally that the nonlinear susceptibility was proportional to  $(\nu - \nu_0)^{-3}$ . This result is obtained from either adiabatic following or the steady-state model.

The term adiabatic following describes the situation in which the pseudomoment  $\vec{p}$  of the near-resonant transition follows (remains parallel to) the effective field  $\vec{\mathcal{E}}_e$  of the laser pulse.<sup>4,7,8</sup> Adiabatic following occurs when two conditions are satisfied. First, in the rotating coordinate frame, the direction of  $\vec{\mathcal{E}}_e$  must change slowly compared to the precession frequency  $\Delta$  of  $\vec{p}$  about  $\vec{\mathcal{E}}_e$  ( $\vec{\mathcal{E}}_e$  must change adiabatically)<sup>9</sup>; second, the pulse width must be short compared to  $T_1$  and  $T_2$  of the atomic system. The response time of  $\vec{p}$  and of the corresponding resonant electronic nonlinearity to changes in  $\vec{\mathcal{E}}_e$  is of the order of  $\Delta^{-1}$  (for the work reported here the response time was less than 100 psec). In contrast to adiabatic following, the steady-state model is insensitive to how the pulse is applied and requires the pulse duration be long compared to both  $T_1$  and  $T_2$ . The response time for the steady-state model is approximately  $T_1$ .

We will now derive the condition for adiabatic